SINTEF
PROCEEDINGS
1

Selected papers from 10th International Conference on Computational Fluid Dynamics in the Oil & Gas, Metallurgical and Process Industries

# Progress in Applied CFD

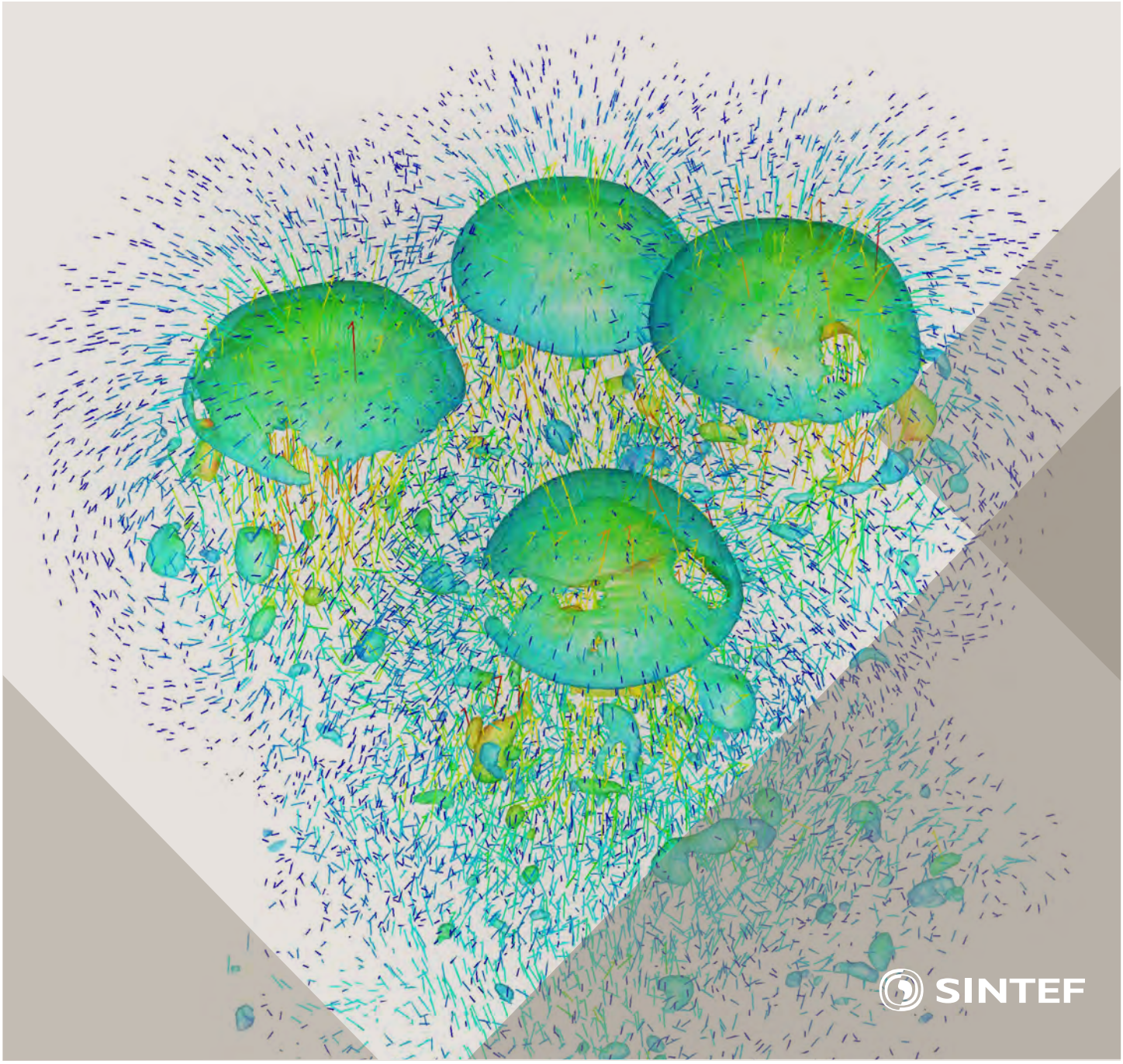

SINTEF Proceedings

Editors:
Jan Erik Olsen and Stein Tore Johansen

# Progress in Applied CFD

Selected papers from 10th International Conference on Computational Fluid Dynamics in the Oil & Gas, Metallurgical and Process Industries

SINTEF Academic Press

SINTEF Proceedings no 1
Editors: Jan Erik Olsen and Stein Tore Johansen
**Progress in Applied CFD**
Selected papers from 10th International Conference on Computational Fluid Dynamics in the Oil & Gas, Metallurgical and Process Industries

Key words:
CFD, Flow, Modelling

Cover, illustration: Rising bubbles by Schalk Cloete

ISSN 2387-4287 (printed)
ISSN 2387-4295 (online)
ISBN 978-82-536-1432-8 (printed)
ISBN 978-82-536-1433-5 (pdf)

60 copies printed by AIT AS e-dit
Content: 100 g munken polar
Cover: 240 g trucard



SINTEF Academic Press
Address: Forskningsveien 3 B
PO Box 124 Blindern
N-0314 OSLO
Tel: +47 22 96 55 55
Fax: +47 22 96 55 08

www.sintef.no/byggforsk
www.sintefbok.no

**SINTEF Proceedings**
SINTEF Proceedings is a serial publication for peer-reviewed conference proceedings on a variety of scientific topics.
The processes of peer-reviewing of papers published in SINTEF Proceedings are administered by the conference organizers and proceedings editors. Detailed procedures will vary according to custom and practice in each scientific community.

## PREFACE

This book contains selected papers from the 10th International Conference on Computational Fluid Dynamics in the Oil & Gas, Metallurgical and Process Industries. The conference was hosted by SINTEF in Trondheim in June 2014 and is also known as CFD2014 for short. The conference series was initiated by CSIRO and Phil Schwarz in 1997. So far the conference has been alternating between CSIRO in Melbourne and SINTEF in Trondheim. The conferences focus on the application of CFD in the oil and gas industries, metal production, mineral processing, power generation, chemicals and other process industries. The papers in the conference proceedings and this book demonstrate the current progress in applied CFD.

The conference papers undergo a review process involving two experts. Only papers accepted by the reviewers are presented in the conference proceedings. More than 100 papers were presented at the conference. Of these papers, 27 were chosen for this book and reviewed once more before being approved. These are well received papers fitting the scope of the book which has a slightly more focused scope than the conference. As many other good papers were presented at the conference, the interested reader is also encouraged to study the proceedings of the conference.

The organizing committee would like to thank everyone who has helped with paper review, those who promoted the conference and all authors who have submitted scientific contributions. We are also grateful for the support from the conference sponsors: FACE (the multiphase flow assurance centre), Total, ANSYS, CD-Adapco, Ascomp, Statoil and Elkem.

Stein Tore Johansen & Jan Erik Olsen

Organizing committee:

Conference chairman: Prof. Stein Tore Johansen
Conference coordinator: Dr. Jan Erik Olsen
Dr. Kristian Etienne Einarsrud
Dr. Shahriar Amini
Dr. Ernst Meese
Dr. Paal Skjetne
Dr. Martin Larsson
Dr. Peter Witt, CSIRO

Scientific committee:

J.A.M.Kuipers, TU Eindhoven
Olivier Simonin, IMFT/INP Toulouse
Akio Tomiyama, Kobe University
Sanjoy Banerjee, City College of New York
Phil Schwarz, CSIRO
Harald Laux, Osram
Josip Zoric, SINTEF
Jos Derksen, University of Aberdeen
Dieter Bothe, TU Darmstadt
Dmitry Eskin, Schlumberger
Djamel Lakehal, ASCOMP
Pär Jonsson, KTH
Ruben Shulkes, Statoil
Chris Thompson, Cranfield University
Jinghai Li, Chinese Academy of Science
Stefan Pirker, Johannes Kepler Univ.
Bernhard Müller, NTNU
Stein Tore Johansen, SINTEF
Markus Braun, ANSYS

## CONTENTS

# Simulation of two-phase viscous oil flow

**Stein Tore JOHANSEN[1,3]*, Sjur MO[1], Jørn KJØLAAS[2], Christian BREKKEN[2] and Ivar ESKERUD SMITH[2]**
[1]SINTEF Materials and Chemistry, 7465 Trondheim, NORWAY
[2]SINTEF Petroleum, 7465 Trondheim, NORWAY
[3]NTNU, Energy & Process Engineering, 7491 Trondheim, NORWAY

* E-mail: Stein.T.Johansen@sintef.no

## ABSTRACT

Multiphase flows of heavy oils and other fluids with high apparent viscosity is a particular industrial challenge. Main challenges here is that interfacial waves, atomization at the large scale gas–liquid interface as well as bubble entrainment and separation all are significantly modified by high fluid viscosity. In addition the viscous liquid may behave as laminar while gas and other low viscosity liquids show turbulent behaviour. Accordingly, correct modelling of the turbulence, including correct transitional behaviour between turbulent and laminar flow becomes of great importance.

In this paper we have investigated two phase flows of gas at a rather high density and viscous oil. Experiments have been performed at the SINTEF Multiphase Flow Laboratory at Tiller, Trondheim. The experimental section was horizontal, with a pipe inner diameter of 69 mm. Pressure drop - and liquid hold-up time series, as well as video-documentation of the flow, were recorded.

The experiments have been analysed and simulated by the Quasi-3D flow model which has been developed in the LedaFlow development project. The results show that flow regimes are well predicted, as well as liquid fractions (hold-up) and pressure drops. Furthermore, some cases have been identified where the Quasi-3D concept is challenged and where the full 3D effects need special attention and modelling.

In the paper we describe the experiments in more details, discuss the general challenges on viscous flow modelling, present the special features of our Quasi-3D flow model and compare predictions to the experimental results. Finally we discuss the perspectives of multidimensional modelling as a virtual laboratory for multiphase pipe flows comprising viscous liquids.

**Keywords:** Two phase pipe flow, viscous fluid, turbulence, laminar-turbulence transition, Quasi-3D modelling

## NOMENCLATURE

*Greek Symbols*

| | | |
|---|---|---|
| $\alpha$ | Volume fraction | [-] |
| $\varepsilon$ | Wall roughness | [m] |
| $\varepsilon_m$ | Turbulent dissipation for phase m | [m$^2$/s$^3$] |
| $\kappa$ | Von Karman Constant (≈ 0.4) | |
| $\mu_m$ | Molecular viscosity for phase m | [Pa·s] |
| $\mu_m^T$ | Turbulent viscosity for phase m | [Pa·s] |
| $\rho_m$ | Density for phase m | [kg/m$^3$] |
| $\theta$ | Pipe inclination | [°] |

*Latin Symbols*

| | | |
|---|---|---|
| $D$ | Pipe diameter | [m] |
| $Fr$ | Froude number ( $Fr = v_{drift} \Big/ \sqrt{gD}$ ) | |
| $v_{drift}$ | Drift velocity, $v_{drift} = U_g - U_o$ | [m/s] |
| $g$ | Gravity (9.81 m/s$^2$) | [m/s$^2$] |
| $k_m$ | Turbulent kinetic energy for phase *m* | [m$^2$/s$^2$] |
| $\ell$ | Turbulent length scale | [m] |
| $L$ | Pipe length | [m] |
| $R$ | Pipe radius | [m] |
| $\mathrm{Re}_g$ | Gas Reynolds number ( $\mathrm{Re}_g = \frac{\rho_g U_{sg} D}{\mu_g}$ ) | |
| $\mathrm{Re}_l$ | Liquid Reynolds number ( $\mathrm{Re}_l = \frac{\rho_l U_{sl} D}{\mu_l}$ ) | |
| $U_k$ | Stream wise velocity for phase k | [m/s] |
| $U_{sk}$ | Stream wise superficial velocity for phase k ( $U_{sk} = \alpha_k U_k$ ) | [m/s] |
| $x$ | Axial distance | [m] |
| $y$ | Transversal distance | [m] |
| $\Delta x, \Delta y$ | Mesh spacing | [m] |

*Sub/superscripts*

*g* gas
*l* liquid
*crit* critical

## INTRODUCTION

Multiphase flows containing viscous fluids appear in many oil and gas applications. Heavy oil contains large molecules and precipitates which result in a viscosity which often is strongly temperature dependent and in some cases may lead to non-Newtonian behaviour. By heating such fluids they may be transported easily as long as the temperature is kept high. However, in some cases heating and excessive insulation is very expensive and it is desirable to transport the fluids at approximately ambient temperature. Evaluation of the feasibility of such transport would rely on accurate flow models.

A special challenge here is that an oil phase at high viscosity may flow as laminar while the remaining phases (gas, water) may show turbulent behaviour. In addition, the interface structures, drainage of liquid wall films, entrainment processes and phase separation are all significantly modified by a high liquid viscosity.

Another challenge is that availability of high quality experimental data from multiphase flow in pipes larger than 2 inches is extremely scarce (Zhang et al., 2012). However, for pipe diameters less than 2 inches surface tension and wall wetting effects play a more significant role than in larger and industrial size pipes. Of the few experiments with somewhat larger pipe diameters we find Gokcal (Gokcal, 2005, Gokcal, 2008), who performed experiments in a 19 m long horizontal flow loop with inner diameter 50.8 mm. He used air and a viscous oil, where the oil viscosity varied from about 180 to 600 cP.

In a literature review (Zhang et al., 2012) it was commented that more experiments and physical models are needed in order to have appropriate understanding and good 1D model predictions. Improving the understanding of such gas/liquid flow is a major motivation of this paper.
In the paper we will discuss the capability of a multidimensional Quasi-3D model (Laux et al., 2007, Mo et al., 2012, Mo et al., 2013b, Mo et al., 2013a) in predicting this type of viscous two phase gas/liquid flows. Detailed experimental data, to be used to understand the physics and benchmark the model, has been recorded at the SINTEF Multiphase Flow facility at Tiller, outside Trondheim. This is further explained in the next section.

## EXPERIMENTS

In the experiments we apply a horizontal pipe with 69 mm ID, and a test section which is 51.4 m. As the experimental loop is indoor, the fluid temperature was monitored and was kept quite constant, with less than 0.1 °C variations during one experiment. The fluid temperature in the test section varied between 18 and 23 °C between experiments. The experimental setup has been documented by (Eskerud Smith et al., 2011). In addition to the instrumentation (broad band gamma densitometers, pressure sensors) we have applied a traversing gamma densitometer. This instrument can record a statistically averaged liquid distribution across the pipe cross section.
From a larger set of two-phase experiments a subset was selected. These data is characterized by a gas/liquid density ratio of approximately 0.05 and a gas/liquid viscosity ratio of approximately 1.5e-4. The surface tension was measured to 0.02 N/m. The oil viscosity itself was in the range of 0.08 – 0.11 Pa·s, which is approximately 100 times more viscous than water. The experimental matrix with summarized overall experimental results is found in Table 1.

**Table 1 Experimental matrix with measured liquid holdup and pressure drop.**

| Exp. ID | Re_liq | Re_gas | Liquid holdup [-] | Pressure gradient [Pa/m] |
|---|---|---|---|---|
| **he10671** | 6.15E+02 | 1.03E+05 | **0.82** | -506 |
| **he10643** | 6.12E+02 | 2.16E+05 | **0.63** | -672 |
| **he11011** | 4.71E+02 | 4.32E+05 | **0.63** | -746 |
| **he11013** | 4.92E+02 | 6.47E+05 | **0.52** | -944 |
| **he10656** | 5.93E+02 | 8.64E+05 | **0.44** | -1012 |
| **he10619** | 5.83E+02 | 1.08E+06 | **0.39** | -1235 |
| **he10627** | 5.97E+02 | 1.30E+06 | **0.30** | -1684 |
| **he11014** | 5.07E+02 | 1.51E+06 | **0.29** | -1997 |
| **he11015** | 5.06E+02 | 1.73E+06 | **0.24** | -2081 |
| **he11016** | 5.11E+02 | 1.94E+06 | **0.20** | -2227 |

The Reynolds numbers in the table are based on the superficial velocity. We see that for an approximately constant liquid Reynolds number ($Re_l$) the liquid fraction decreases significantly with increased gas Reynolds number ($Re_g$). As a consequence, the liquid phase velocity has increased by a factor of approximately 4 for the highest gas flow rate. Hence, as the gas Reynolds number increases the liquid will pass through the transition from laminar to turbulent liquid flow. This is a result of an increasing liquid Reynolds number based on the hydraulic diameter and phase velocity of the liquid. At the same time the pressure drop increases strongly with increasing gas flow rate.
More details about the experimental results are given in the result section, after introducing the flow model.

## MODEL DESCRIPTION

### Model basis

The flow model is based on a 3D and 3-phase formulation, where the equations are derived based on volume averaging and ensemble averaging of the Navier-Stokes equations. Conceptually, the model is based on the following elements (Laux et al., 2007). A multi-fluid Eulerian model allowing two types of dispersed fields[1] in each of the three continuous fluids.

[1] Each phase can appear as different fields. For a 3-phase situation each phase may be continuous or dispersed in each of the other continuous phases.

i) The flow domain consists of several zones, each with a well-defined continuous fluid, separated by Large Scale Interfaces (LSIs)
ii) Between the zones local boundary conditions are applied (interface fluxes)
iii) A field based turbulence model with wall functions for LSIs and solid walls.
iv) Evolution models for droplet- and bubble sizes
v) By adding together the field-based equations for each phase, phase based mass-, momentum-, and turbulence equations are obtained

At the LSIs we use the concept of wall functions, where the shear stresses from both sides of the interface are approximated by the wall functions for rough walls (Ashrafian and Johansen, 2007). The same wall functions are used to calculate the added turbulence production in LSI cells. The effect of non-resolved waves is modelled by a density corrected Charnock model (Charnock, 1955). The use of wall functions at the LSIs is supported by e.g. (Bye and Wolff, 2007) studying the air-sea interface.

The turbulence is modelled using a $k-\ell$ model where k is the turbulent kinetic energy and $\ell$ is a turbulent mixing length scale based on flow domain geometry. The length scale is solved from a Poisson equation where the length scale at solid walls and LSIs are related to roughness and given as boundary conditions:

$$\nabla^2 \ell = -\frac{\kappa}{R} \qquad (1)$$

Here κ is the von Karman constant and R is the pipe radius. The length scale in cells near walls and LSIs are given by algebraic relations. The turbulent kinetic energy equations are solved for each phase by applying wall laws at solid walls and the LSIs. The turbulent viscosity for phase m is given by:

$$\mu_m^T = \rho_m \ell \left(0.35 k_m\right)^{1/2} \qquad (2)$$

where $\rho_m$ is density and $k_m$ is turbulent kinetic energy for phase m. The turbulent dissipation rate for phase m is:

$$\varepsilon_m = \frac{\left(0.35 k_m\right)^{3/2}}{\ell} \qquad (3)$$

The resulting model gives the volume fractions and velocity (momentum) for the phases in the flow. In order to apply local boundary conditions inside the flow as described above we need to identify the LSIs. This is done based on an evaluation of the predicted phase volume fraction, based on the assumption that there is a critical volume fraction which controls phase inversion. In this work a phase is assumed continuous if the local volume fraction in a computational cell is above a critical volume fraction $\alpha_{crit} = 0.5$. Based on a relatively simple reconstruction algorithm, the interface is reconstructed such that the local boundary conditions can be applied. Presently, the effects of surface tension on the motion of the LSI are not included. This simplification is valid as long as we use relatively coarse grids and do not want to resolve capillary waves. This model framework has the capability to handle any 3-phase (or less) multiphase flow as long as the flow can be described by 9 fields – 3 continuous fields with 2 dispersed fields in each. As this model is directed towards applications such as predictions of multiphase flows in pipelines the target is to simulate reasonably long sections of pipes for considerable flow-times. This restriction demands simplifications in order to be able to obtain results in a reasonable CPU time. Weeks or months of computer time on parallel machines would not be acceptable for most industrial applications. The simplification we have introduced is the Quasi-3D (Q3D) approximation. By slicing the pipe in one direction, normal to the pipe axis, (usually the vertical direction), as demonstrated in Figure 1, the flow can be resolved on a 2-dimensional mesh, but still keeping important aspects from the 3D pipe geometry.

The full 3D model equations are then averaged over the transversal distance to create slice averaged model equations. In this process the 3D structures are homogenized and the flow becomes represented by slice averaged fields. One result is that the wall fluxes, such as shear stresses, becomes source terms in what we call Quasi-3D (Q3D) model equations (for details, see (Laux et al., 2007)). It should be noted that the length scale equation (1) is solved using the 2D Laplacian in the x-y plane (Figure 1).

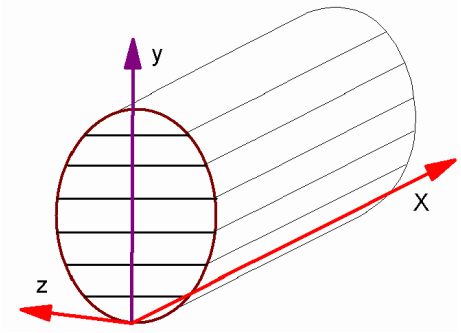


Figure 1 Quasi 3D grid cells, showing one axial (x-direction) and seven vertical cells (y-direction). The z-direction is averaged over to get Q3D equations.

The numerical solution is performed on a staggered Cartesian mesh, where the discrete mass, pressure and momentum equations are solved by an extended phase-coupled SIMPLE method (for details, see e.g. (Patankar, 1980)). The implicit solver uses first order-time discretization and up to third-order in space for convective terms (Laux et al., 2007).

The Quasi 3D model description is expected to perform well in horizontal stratified and hydrodynamic slug flows where the large scale interface is dominantly horizontal at a given axial position x, as seen in Figure 1 and demonstrated in previous papers (Laux et al., 2008a, Laux et al., 2008b, Laux et al., 2007).

The applicability of the Q3D approximation to horizontal gas liquid flows with high liquid viscosity

will be discussed next. We note that the model has not included a field for the thin liquid film which is drained by gravity after passage of waves or slugs. Adding such a field with separate momentum- and mass conservation equations may be necessary in the case when the liquid is extremely viscous.

## Simulations

Based on the 10 flow situations, represented by Table 1, 10 flow cases were defined. The length of the simulated domain was 20 meters, with diameter 69 mm. The applied grid comprised 20 (transversal) x 1000 (axial) grid points. Thus, the grid aspect ratio is 5.8.

The simulations were run for 60 seconds real time, and data from the last 30 seconds were applied to calculate statistics from the simulations. The total simulation time spanned from approximately 4 to 30 times the fluid residence time in the flow domain. By further inspection of the data it was verified that the last 30 seconds should give a good representation of the capability of the model. At the flow inlet the flow was in all cases assumed stratified (liquid fraction of 0.4), with no dispersed droplets and bubbles. The inlet turbulent energy was set to 0.001 $m^2/s^2$. The model has several physical constants related to the bubble- and droplet transport models (Mo et al., 2013b), which are given in Table 2. Wave roughness is characterized by the Charnock constant (used default value of 10) and the dispersed phase concentrations at the Large Scale Interface are set to 0.3.

**Table 2 Model constants for the size of dispersed fields (Mo et al., 2013b).**

| | C1 | C2 | C3 | C4 |
|---|---|---|---|---|
| Bubbles | 10 | 0.1 | 1.00E-05 | 0.1 |
| Droplets | 0.02 | 0.002 | 1.00E-06 | 0.1 |

## RESULTS

### *Pressure drop and liquid holdup*

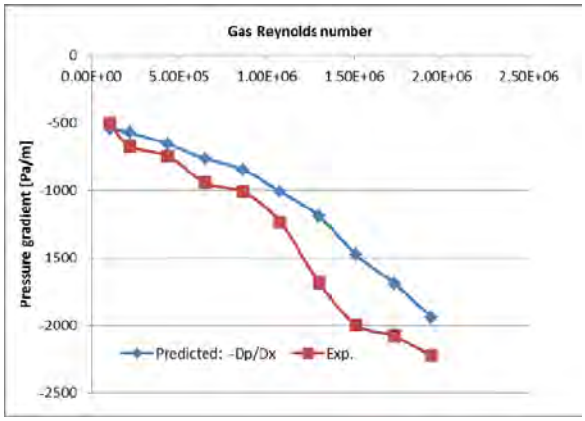


**Figure 2 Predicted- and experimental pressure gradient versus gas Reynolds number.**

The time averaged pressure drop was calculated over the last 50% of the pipe length. The predicted and experimental pressure drops are compared in Figure 2. We see that for the lowest velocity the model and experiments compare well. With increased flow velocity we see a consistent under-prediction of the pressure drop, not exceeding 30%. The under-prediction is quite systematic, but with a good qualitative trend.

The liquid holdup was calculated at a position 95% of the pipe length from the inlet. The results are shown in Figure 3, where we see that holdup is well reproduced for the entire velocity range. For the lowest gas Reynolds numbers we see some under-prediction of the liquid holdup. This can also be seen as an over-prediction of the gas velocity. The overall comparison is very good, both qualitative and quantitative.

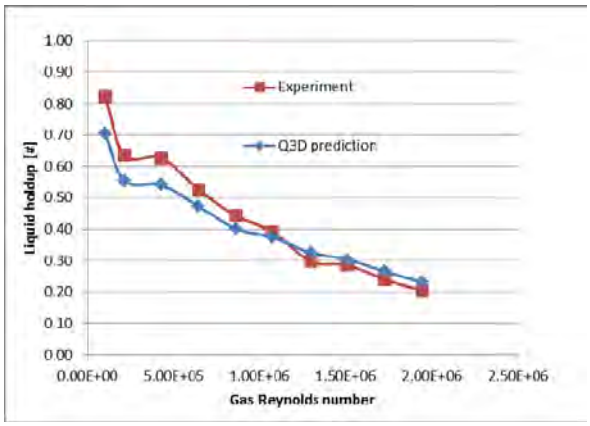


**Figure 3 Predicted- and experimental liquid holdup versus gas Reynolds number.**

### *Dynamic performance of the liquid holdup*

The liquid holdup (fraction) was measured dynamically with a broad band gamma densitometer. In Figure 4 we see the comparison between the predicted- and experimental time traces of the liquid holdup, for all the cases, and where the ID codes refer to Table 1. We see that the two cases with lowest gas velocity have a typical slug type time trace. This is reproduced by the model, but the variations in the liquid fraction are larger in the predictions than in the experiments. In other words, the bubbles in the experiments are shallower than in the model.

With increasing gas velocities (moving upwards in the figure) the flow becomes more stratified, with lower amplitude in the liquid holdup oscillations. These trends are by large captured by the model. However, from the figure we have an indication that the Q3D model produces more large scale waves than observed in the experiment. We may note that for both experiments and simulations the data sampling interval is 0.1 sec. In the high gas velocity cases, such as he100671, the liquid velocity is approximately 5 m/s and only waves larger than 0.5 m are possible to resolve by the gamma densitometer (due to time averaging). However, the Q3D model reports the instantaneous results on the 20 mm grid. A better comparison would be to smooth the prediction results in the same manner as the gamma densitometer works. Then the simulation results would look smoother for the high flow rate cases.

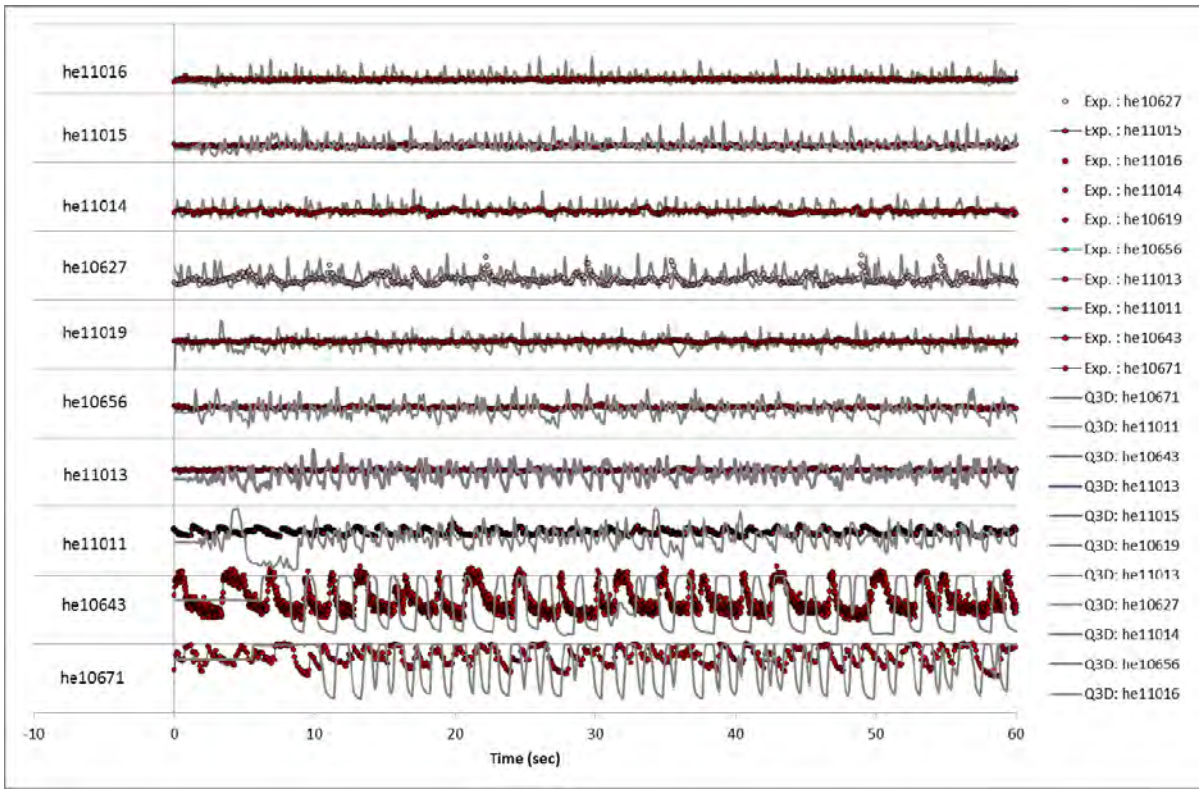


**Figure 4 Predicted- versus experimental time traces of the liquid holdup for all 10 cases studied. The ID codes refer to Table 1. The gas velocity increases from bottom to top.**

*Flow structures and statistics*

In Figure 5 to Figure 14 we show snap shots of the liquid distribution (red colour) for the different gas Reynolds numbers. Note that the diameter is increased by a factor four in the figures for visibility. Regions with yellow colour indicate high amounts (∼25%) of dispersed gas entrained into the liquid. Case IDs are defined in Table 1, and the gas velocity increases by increasing figure number. In addition the figures show the comparison between the experimental and predicted vertical distribution of the liquid. Note that for the experiments (blue lines) the scatter around the average liquid fraction is a combination of the variations on the physical volume fraction and the nature of the narrow band gamma instrument. The predicted profiles are extracted from position 95% of the pipe length (19 m).

What we see from the figures is that for the two lower gas flow rate cases (he10671 and he10643) the flow regime is slug flow. However, the predicted liquid profile does not agree well with the experimental liquid distribution in Figure 5, verifying that the predicted spreading of the large bubbles over the pipe cross section is not in accordance with the experiments. A main explanation for this is that our model is slice-averaged over the width of the pipe. The additional dispersion due to different velocities in the cross section is not included in the model. In turbulent flows this approximation is very good. However, in the present two cases the liquid is laminar and the reduced dispersion due to the dimension reduction has clearly some impact on the prediction. Still, both predicted pressure drop and holdup must be seen as acceptable.

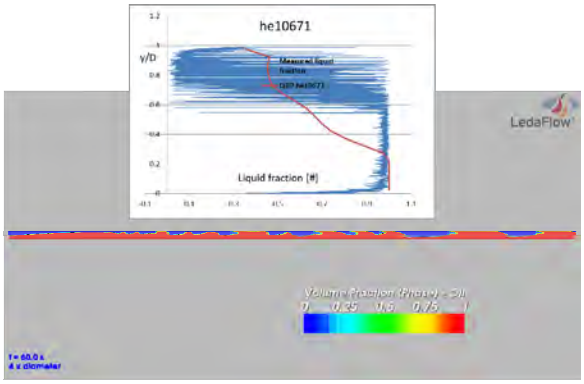


**Figure 5 Case he10671: Snap shot of oil fraction. Insert shows predicted versus experimental ensemble averaged profile of vertical liquid holdup distribution.**

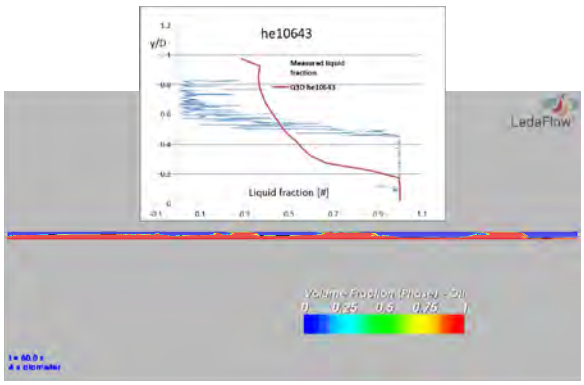


**Figure 6 Case he10643: Snap shot of oil fraction. Insert shows predicted versus experimental ensemble averaged profile of vertical liquid holdup distribution.**

For the cases he11011 to he10619 (Figure 7 to Figure 10) we see that our model is producing more waves than what can be supported from the traversing gamma holdup profiles. The reason for the relatively poor qualitative prediction of the liquid distribution seen in a case like he11013 is not clear. In an almost parallel experiment (he10648, not shown here) the predicted profile is much closer to the experiments. At the moment we do not have a good explanation why the experimental flow is much more stable than in the simulation. One possibility is that the effective friction at the Large Scale interface (LSI) is not accurate for this flow range, impacting the interface stability. At the same time the overall interface friction must be rather well reproduced due to the good prediction of liquid holdup. Understanding the combined role of droplet momentum exchange, wall and interface friction will need further investigations.

From case he10627 (Figure 11) and onwards (until Figure 12), we see that distribution of the liquid over the pipe cross section is rather well reproduced. For the three largest gas Reynolds numbers the comparison is very good. It is interesting to note that for these flow cases we have significant amounts of entrained bubbles (shown by the yellow regions).

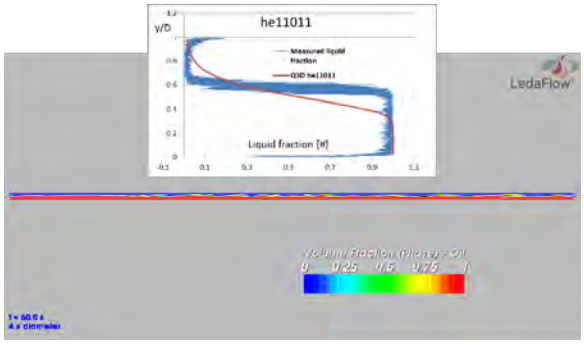


**Figure 7 Case he11011: Snap shot of oil fraction. Insert shows predicted versus experimental ensemble averaged profile of vertical liquid holdup distribution.**

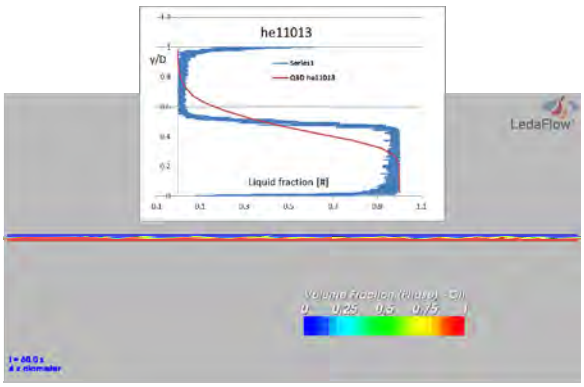


**Figure 8 Case he11013: Snap shot of oil fraction. Insert shows predicted versus experimental ensemble averaged profile of vertical liquid holdup distribution.**

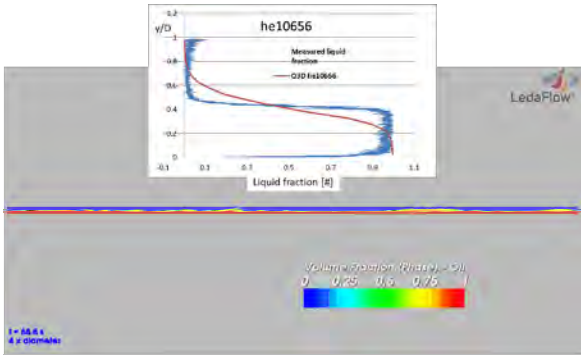


**Figure 9 Case he10656: Snap shot of oil fraction. Insert shows predicted versus experimental ensemble averaged profile of vertical liquid holdup distribution.**

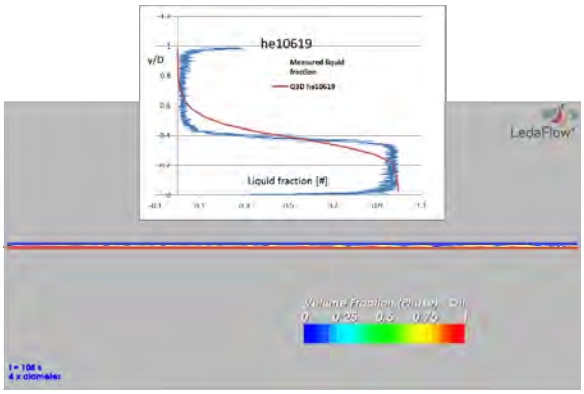


**Figure 10 Case he10619: Snap shot of oil fraction. Insert shows predicted versus experimental ensemble averaged profile of vertical liquid holdup distribution.**

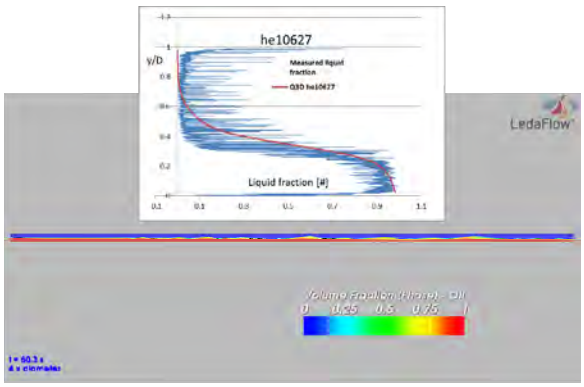


**Figure 11 Case he10627: Snap shot of oil fraction. Insert shows predicted versus experimental ensemble averaged profile of vertical liquid holdup distribution.**

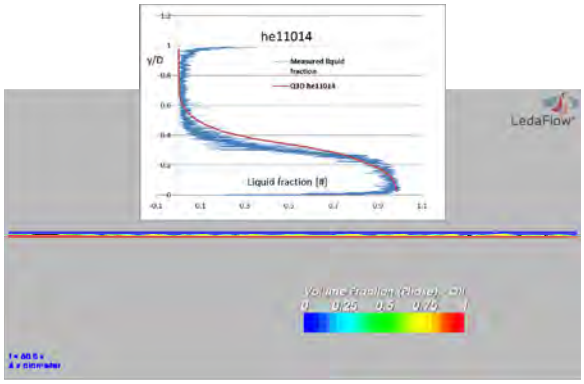


**Figure 12 Case he11014: Snap shot of oil fraction. Insert shows predicted versus experimental ensemble averaged profile of vertical liquid holdup distribution.**

*Grid dependency*

Introductory simulations with 15 and 20 grid points over the pipe cross section indicated that some improvements of the resolution of waves were achieved by going to 20 cells. The axial grid was tested at 500, 1000 and 2000 grid points. The 500 axial grid points led to suppression of waves. One case (he11014) was run using 2000 axial points. The predicted vertical profiles of the liquid holdup could not visually be distinguished from the case using 1000 point.

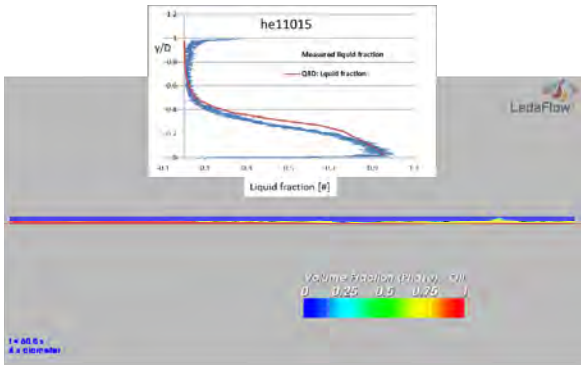


**Figure 13 Case he11015: Snap shot of oil fraction. Insert shows predicted versus experimental ensemble averaged profile of vertical liquid holdup distribution.**

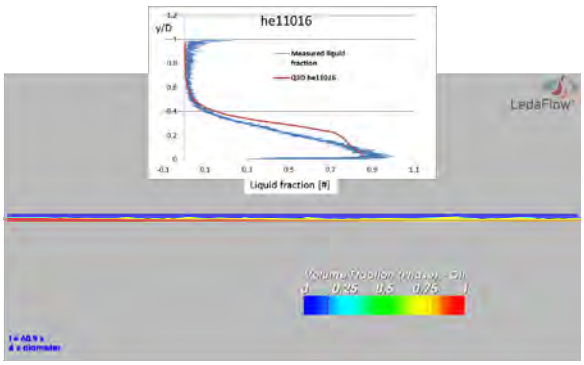


**Figure 14 Case he11016: Snap shot of oil fraction. Insert shows predicted versus experimental ensemble averaged profile of vertical liquid holdup distribution.**

*Developed flow*

The length needed to develop the flow depends on several physical phenomena, especially the entrainment and coalescence and separation of entrained bubbles. The development length will in general be longer at higher velocities since bubble coalescence time scales can be quite long. In general, the flow has been developed to a quite developed state, as seen in Figure 15. What we see here is representative for all the simulations. By doubling the length of the flow domain only marginal improvements can be expected.

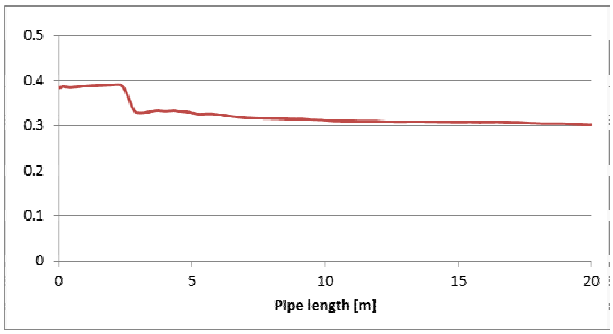


**Figure 15 Time averaged liquid holdup versus length of simulated pipe (Case he11014).**

## CONCLUSIONS

Horizontal two-phase gas-liquid flow with a highly viscous liquid was simulated using a Quasi-3D flow model. Even if the model is reduced from 3D to 2D the prediction power of the model is good. The liquid holdup is very well predicted while the pressure drop shows a systematic under-prediction. Parts of this under-prediction may be due to an increased effective viscosity due to entrained micro-bubbles in the oil phase. Still the qualitative change in liquid holdup and pressure drop versus gas flow rate is very well reproduced, and the gas Reynolds number for transition between slug-flow and stratified flow is predicted accurately.

From liquid holdup time traces and comparisons with the traversing gamma experiments it was found that during slug flow the bubble shape is not correctly reproduced by the model. This is a result of the

predominantly laminar flow in the liquid and strong variation in the liquid velocity within one computational cell (slice). In order to account for this effect a Taylor type dispersion mechanism must be included in the model. Even if the bubble propagation was not correctly predicted the quantitative prediction of pressure drop and liquid fraction was both better than $\pm 15\%$.

For the higher gas flow rates ($Re_g > 10^6$) it was found that the Q3D model predicts very well both the quantitative and qualitative flow behaviour.

It should be noted that the model was run without trying to improve on the model coefficients. With this in mind, it is clear that the Q3D model is capable of predicting viscous gas-liquid two-phase flows. Based on our findings we realize that the Q3D model has a significant potential to become a numerical laboratory for interpretation and extension of experimental data, and can in addition serve as a means to deduce closure laws for simplified 1D models.

A natural extension of this work is to investigate the performance of the Q3D model for inclined and vertical two-phase flows, and as a further step extend the investigation to three-phase flows. Already now we realize that access to high quality experiments including cross-sectional profiles will be crucial for such a development.

## ACKNOWLEDGEMENTS

The financial support to the Leda Project, the long-time contributions from the Leda Technical Advisory Committee, as well as permission to publish, by Total, ConocoPhillips, and SINTEF are all gratefully acknowledged. Our colleagues Ernst Meese, and Runar Holdahl (SINTEF), Wouter Dijkhuizen and Dadan Darmana (Kongsberg Oil & Gas Technologies), Harald Laux (OSRAM Opto Semiconductors GmbH, Regensburg), and Alain Line (INSA, Toulouse) are acknowledged for their contributions to the development.

## REFERENCES

ASHRAFIAN, A. & JOHANSEN, S. T. 2007. Wall boundary conditions for rough walls. *Progress in Computational Fluid Dynamics,* 7**,** 230-236.

BYE, J. A. T. & WOLFF, J.-O. 2007. Charnock dynamics: a model for the velocity structure in the wave boundary layer of the air-sea interface. *Ocean Dynamics,* 58**,** 31-42.

CHARNOCK, H. 1955. Wind stress on a water surface. *Quart J Roy Meteor Soc,* 81**,** 639-40.

ESKERUD SMITH, I., KRAMPA, F. N., FOSSEN, M., BREKKEN, C. & UNANDER , T. E. Investigation of Horizontal Two-Phase Gas-Liquid Pipe Flow Using High Viscosity Oil: Comparison with Experiments Using Low Viscosity Oil and Simulations. 2011. BHR Group 2011 Multiphase 15, 2011 Cannes, France. BHR Group.

GOKCAL, B. 2005. *Effects of high oil viscosity on two-phase oil-gas flow behavior in horizontal pipes.* Master of Science, University of Tulsa.

GOKCAL, B. 2008. *An experimental and theoretical investigation of slug flow for high oil viscosity in horizontal pipes. Ph.D. Dissertation,.* PhD, The University of Tulsa.

LAUX, H., MEESE, E., JOHANSEN, S. T., LADAM, Y., BANSAL , K. A., DANIELSON, T. J., GOLDSZAL, A. & MONSEN, J. I. 2007 Simulation of multiphase flows composed of large scale interfaces and dispersed fields. Int. Conf. Multiphase Flows, 2007 Leipzig.

LAUX, H., MEESE, E. A., MO, S., JOHANSEN, S. T., BANSAL, K. M., DANIELSON, T. J., GOLDSZAL, A. & MONSEN, J. I. Multi-dimensional simulations of slug and slug-like flows in inclined pipes and channels. OTC 2008a Houston. 21-37.

LAUX, H., MEESE, E. A., MO, S., UNANDER, T. E., JOHANSEN, S. T., BANSAL, K. M., DANIELSON, T. J., GOLDSZAL, A. & MONSEN, J. I. 2008b. Multidimensional Simulations of Multiphase Flow for Improved Design and Management of Production and Processing Operation. *2008 Offshore Technology Conference.* Houston, Texas, U.S.A: SPE.

MO, S., ASHRAFIAN, A., BARBIER, J.-C. & JOHANSEN, S. T. Quasi-3D modelling of two-phase slug flow in pipes. Ninth International Conference on CFD in the Minerals and Process Industries, CSIRO, 2012 Melbourne, Australia, 10-12 December

MO, S., ASHRAFIAN, A. & JOHANSEN, S. T. 2013a. Simulation of flow regime transitions in vertical pipe flow. *8th International Conference on Multiphase Flow, ICMF2013.* Jeju, Korea.

MO, S., ASHRAFIAN, A. & JOHANSEN, S. T. 2013b. Two phase flow prediction of fluid displacement operations. *8th International Conference on Multiphase Flow, ICMF 2013.* Jeju, Korea.

PATANKAR, S. V. 1980. *Numerical Heat Transfer and Fluid Flow*, New York, McGraw-Hill Book Company.

RØNNINGSEN, H. P. 2012. Rheology of petroleum fluids. *Annual Transactions of the Nordic Rheology Society,* 20**,** 11-18.

ZHANG, H.-Q., SARICA, C. & PEREYRA, E. 2012. Review of High-Viscosity Oil Multiphase Pipe Flow. *Energy & Fuels,* 26**,** 3979-3985.